Oxygen Nonstoichiometry in $YBaCo_4O_{7+\delta}$: Large Low-Temperature Oxygen Absorption/Desorption Capability

M. Karppinen,*,† H. Yamauchi,† S. Otani,† T. Fujita,† T. Motohashi,† Y.-H. Huang,†,§ M. Valkeapää,† and H. Fjellvåg‡

Materials and Structures Laboratory, Tokyo Institute of Technology, Yokohama 226-8503, Japan, and Centre for Materials Science and Nanotechnology, Department of Chemistry, University of Oslo, N-0315 Oslo, Norway

Received October 20, 2005

An uncommon oxygen absorption/desorption behavior is reported for the cation-stoichiometric cobalt oxide, $YBaCo_4O_7$, structurally composed of two kinds of layers of corner-sharing CoO_4 tetrahedra. We have found that $YBaCo_4O_{7+\delta}$ absorbs and desorbs oxygen up to $\delta \approx 1.5$ in a narrow temperature range below 400 °C. The oxygen uptake/release process is highly reversible, being controlled by both temperature and oxygen partial pressure. Such a large low-temperature oxygen-content tunability is of great promise in regard to applications related to, for example, oxygen storage. Materials with similar characteristics are, to a large degree, lacking today.

Introduction

Nonstoichiometric transition metal (T) oxides[1] are important in various fields of modern inorganic material technology. From the structural point of view, oxygen nonstoichiometry may manifest itself in four different ways: (i) interstitial oxygen atoms [in, e.g., Ruddlesden−Popper phases $La_{n+1}T_nO_{3n+1+\delta}$ (T = Cu, Ni, or Co)[2,3]], (ii) cation vacancies (in, e.g., $La_{1-x}Mn_{1-x}O_3$ perovskite[4]), (iii) oxygen vacancies (in, e.g., $YBa_2Cu_3O_{7-\delta}$ and other high-T_c superconductive copper oxides[5,6]), and (iv) interstitial cations (in, e.g., $Zn_{1+x}O$[1]). The first two alternatives result in an overall oxygen excess, whereas the latter two result in an oxygen deficiency.

The technological attractiveness of nonstoichiometric oxides derives from the following unique characteristics. First, oxygen nonstoichiometry is closely related to mixed-valency of the constituent cations and, accordingly, to many important electrofunctional properties such as superconductivity, magnetoresistivity, thermoelectricity, and so forth. Second, the presence of vacant oxygen sites makes it possible for oxide ions to move/diffuse with a reasonable speed in the crystal lattice, as recognized by Nernst[7] more than a century ago and already utilized in applications ranging from solid-oxide fuel cells to gas-separation membranes and oxygen sensors. The material variety[8,9] includes fluorite-structured ZrO_2[7] and CeO_2,[10] the brownmillerite $Ba_2In_2O_5$,[11] the perovskite $LaGaO_3$,[12] the pyrochlore $Gd_2Ti_2O_7$,[13] and the Aurivillius-type phase $Bi_4V_2O_{11}$;[14] though it should be emphasized that lower-for-higher-valence cation substitutions are often required to create a sufficient amount of oxygen vacancies in these cation-stoichiometric phases. (The recently discovered $La_2Mo_2O_9$ oxide-ion conductor is an interesting exception as it intrinsically contains oxygen vacancies.[15]) The third important aspect is that nonstoichiometric oxides are also good candidates for a matrix that allows reversible oxygen charging and discharging (preferably achieved by only modest changes in external conditions). This would—if facilitated at low temperatures—provide us with a "mild" source of highly reactive oxygen that could potentially be used in various chemical and biological processes and technologies.

Here, we report a promising low-temperature oxygen absorption/desorption behavior of the recently discovered cation-stoichiometric cobalt oxide, $YBaCo_4O_7$.[16] The crystal

* Corresponding author fax:+81-45-924-5365; tel: +81-45-924-5333; e-mail: karppinen@msl.titech.ac.jp.
† Tokyo Institute of Technology
‡ University of Oslo
§ Current address: Texas Materials Institute, ETC 9.102, The University of Texas at Austin, Austin, TX 78712.

(1) Sørensen, T. *Nonstoichiometric Oxides*; Academic Press: New York, 1981; p 441.
(2) Jorgensen, J. D.; Dabrowski, B.; Pei, S.; Richards, D. R.; Hinks, D. G. *Phys. Rev. B* **1989**, *40*, 2187.
(3) Fjellvåg, H.; Hansteen, O. H.; Hauback, B. C.; Fischer, P. *J. Mater. Chem.* **2000**, *10*, 749.
(4) Tofield, B. C.; Scott, W. R. *J. Solid State Chem.* **1974**, *10*, 183.
(5) Kishio, K.; Shimoyama, J.; Hasegawa, T.; Kitazawa, K.; Fueki, K. *Jpn. J. Appl. Phys.* **1987**, *26*, L1228.
(6) Karppinen, M.; Yamauchi, H. Oxygen engineering for functional oxide materials. In *International Book Series: Studies of High-Temperature Superconductors*; Narlikar, A. V., Ed.; Nova Science Publishers: New York, 2001; Vol. 37, pp 109−143.
(7) Nernst, W. Material for Electric-Lamp Glowers. U.S. Patent 685730, 1901.
(8) Boivin, J. C.; Mairesse, G. *Chem. Mater.* **1998**, *10*, 2870.
(9) Kharton, V. V.; Marques, F. M. B.; Atkinson, A. *Solid State Ionics* **2004**, *174*, 135.
(10) Tuller, H. L.; Nowick, A. S. *J. Electrochem. Soc.* **1975**, *122*, 255.
(11) Goodenough, J. B.; Ruiz-Diaz, J. E.; Zhen, Y. S. *Solid State Ionics* **1990**, *44*, 21.
(12) Ishihara, T.; Matsuda, H.; Takita, Y. *J. Am. Chem. Soc.* **1994**, *116*, 3801.
(13) Kramer, S. A.; Tuller, H. L. *Solid State Ionics* **1995**, *82*, 15.
(14) Abraham, F.; Boivin, J. C.; Mairesse, G.; Novogrocki, G. *Solid State Ionics* **1990**, *40*−*41*, 934.
(15) Lacorre, P.; Goutenoire, F.; Bohnke, O.; Retoux, R.; Laligant, Y. *Nature* **2000**, *404*, 856.
(16) Valldor, M.; Andersson, M. *Solid State Sci.* **2002**, *4*, 923−931. Valldor, M. *Solid State Sci.* **2004**, *6*, 251.

10.1021/cm0523081 CCC: $33.50
Published on Web 12/16/2005

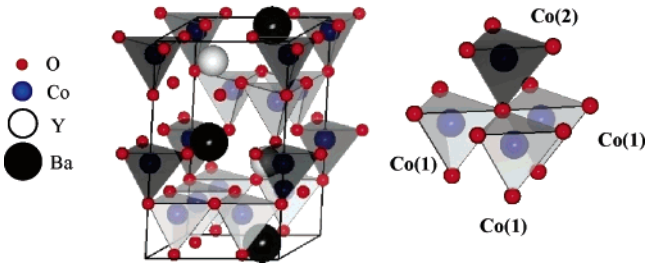

Figure 1. Schematic illustration of the crystal structure of $YBaCo_4O_7$.

structure of $YBaCo_4O_7$ (Figure 1) is similar to that of hexagonal $LuBaAlZn_3O_7$,[17] containing corner-sharing CoO_4 tetrahedra of two kinds with a ratio of 1:3. The two kinds of tetrahedra are distinguished by different sets of bond lengths and located in separate layers that alternate with each other. We have found that $YBaCo_4O_{7+\delta}$ reversibly absorbs and desorbs oxygen up to $\delta \approx 1.5$ in a very narrow temperature range below 400 °C. This oxygen uptake and release capability substantially exceeds both in the overall magnitude and in the response sensitivity those achieved with, for example, various perovskite and Ruddlesden−Popper phases.[2,3,18−24]

Experimental Section

The $YBaCo_4O_{7+\delta}$ samples were synthesized from a precursor powder prepared by an EDTA (ethylenediaminetetraacetic acid) complex gel method[25] using Y_2O_3, $Ba(NO_3)_2$, and $Co(NO_3)_2 \cdot 6H_2O$ as starting materials. The precursor powder was calcined in air at 1000 °C for 10 h, then pelletized and sintered in air at 1200 °C for 24 h. After sintering, the sample pellets were furnace-cooled to room temperature in less than 4 h. Besides the as-air-synthesized samples, two series of samples were prepared by annealing portions of the as-synthesized powder at various temperatures in 1 or 100 atm O_2 for 24 h with a rapid cooling back to room temperature. X-ray powder diffraction (XRD; Rigaku: RINT-2000 equipped with a rotating copper anode; Cu K_α radiation) was used to check the phase purity and lattice parameters of the samples. Moreover, for every sample, the precise oxygen content was determined by iodometric titration[26] from three to five parallel analyses with a reproducibility better than ± 0.01 for δ.

The oxygen absorption/desorption characteristics were investigated by thermogravimetric experiments (TG; Perkin-Elmer: Pyris 1) in O_2, air, and N_2 atmospheres. The mass of the sample was 10∼30 mg, and the heating rate was 1 °C/min. The relatively small sample size and the slow heating rate were selected to guarantee the TG datum at each temperature to represent thermal equilibrium as close as possible. Isothermal TG annealing experiments were carried out in order to investigate the speed of the absorption and desorption processes.

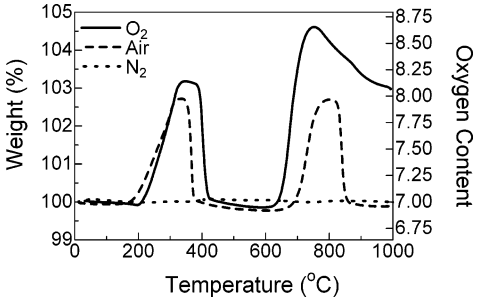

Figure 2. TG curves recorded for as-air-synthesized $YBaCo_4O_{7.01}$ in O_2, air, and N_2 atmospheres (heating rate 1 °C/min).

Representative samples were characterized for transport properties: electrical resistivity (ρ) in the temperature range of 2∼350 K using a standard four-probe technique (Quantum Design: PPMS System-Model 6000) and thermoelectric power or Seebeck coefficient (S) in the temperature range of 150∼300 K with a steady-state technique.

Results and Discussion

All the as-air-synthesized samples were confirmed to be of single phase $YBaCo_4O_{7+\delta}$ within the detection limit of X-ray diffraction. The lattice parameters were readily refined from the X-ray diffraction data in space group $P6_3mc$ with $a = 6.300(1)$ Å and $c = 10.237(1)$ Å, being in good agreement with those given in the first report[16] on this compound. From iodometric titration, the oxygen content was determined as $\delta = 0.01(1)$, which corresponds to the average valence of cobalt, $V(\mathrm{Co})_{av} \approx 2.25$.

Figure 2 presents TG curves recorded for as-synthesized $YBaCo_4O_{7.01}$ upon heating in N_2, air, and O_2 atmospheres. In N_2, the sample weight and, thus, the oxygen content remain unchanged up to 1000 °C (i.e., the maximum temperature reached by our thermobalance). This means that, for the $YBaCo_4O_{7+\delta}$ phase, the oxygen content $7 + \delta \approx 7.00$ represents the minimum. On the other hand, upon heating in O_2-containing atmospheres, the phase was found to absorb considerable amounts of oxygen. The thermograms recorded in air and O_2 both exhibit two prominent humps due to weight gain and subsequent weight loss, the first being around 200∼400 °C, the other around 600∼900 °C (Figure 2).

To clarify the nature of the two humps, we prepared a series of samples by annealing portions of the as-synthesized material at various temperatures in O_2 (for 1∼24 h with a rapid cooling back to room temperature) and recorded XRD patterns for the annealed samples. For a sample annealed at 720 °C in O_2 for 1 h, no diffraction peaks due to the $YBaCo_4O_{7+\delta}$ phase were seen, but the sample contained $BaCoO_{3-\delta}$ as the main phase. Diffraction peaks due to the $BaCoO_{3-\delta}$ phase, though weak, were already seen for a sample annealed at 620 °C for 1 h. We thus conclude that the second weight gain above 600 °C reflects the decomposi-

(17) Rabbow, C.; Müller-Buschbaum, H. *Z. Naturforsch., B: Chem. Sci.* **1996**, *51*, 343. Rabbow, C.; Panzer, S.; Müller-Buschbaum, H. *Z. Naturforsch., B: Chem. Sci.* **1997**, *52*, 546.
(18) MacChesney, J. B.; Sherwood, R. C.; Potter, J. F. *J. Chem. Phys.* **1965**, *43*, 1907.
(19) Negas, T.; Roth, R. S. *J. Solid State Chem.* **1970**, *1*, 409.
(20) Mizusaki, J.; Yamauchi, S.; Fueki, K.; Ishikawa, A. *Solid State Ionics* **1984**, *12*, 119. Mizusaki, J.; Yoshihiro, M.; Yamauchi, S.; Fueki, K. *J. Solid State Chem.* **1985**, *58*, 257. Mizusaki, J.; Mima, Y.; Yamauchi, S.; Fueki, K.; Tagawa, H. *J. Solid State Chem.* **1989**, *80*, 102. Mizusaki, J.; Tagawa, H.; Naraya, K.; Sasamoto, T. *Solid State Ionics* **1991**, *49*, 111. Mizusaki, J. *Solid State Ionics* **1992**, *52*, 79.
(21) Buttrey, D. J.; Ganguly, P.; Honig, J. M.; Rao, C. N. R.; Schartman, R. R.; Subbanna, G. N. *J. Solid State Chem.* **1988**, *74*, 233.
(22) Fjellvåg, H.; Hansteen, O. H.; Tilset, B. G.; Olafsen, A.; Sakai, N.; Seim, H. *Thermochim. Acta* **1995**, *256*, 75.
(23) Karppinen, M.; Yamauchi, H.; Suematsu, H.; Isawa, K.; Nagano, M.; Itti, R.; Fukunaga, O. *J. Solid State Chem.* **1997**, *130*, 213.
(24) Yang, Z. H.; Lin, Y. S. *Ind. Eng. Chem. Res.* **2002**, *41*, 2775. Yang, Z. H.; Lin, Y. S. *Solid State Ionics* **2005**, *176*, 89.
(25) Huang, Y. H.; Lindén, J.; Yamauchi, H.; Karppinen, M. *Chem. Mater.* **2004**, *16*, 4337.
(26) Karppinen, M.; Matvejeff, M.; Salomäki, K.; Yamauchi, H. *J. Mater. Chem.* **2002**, *12*, 1761.

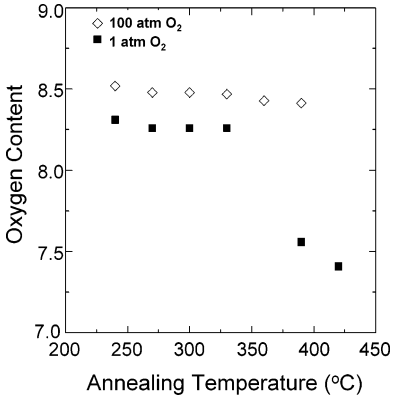

Figure 3. Oxygen-content values (from iodometric titration) for $YBaCo_4O_{7+\delta}$ samples annealed at various temperatures in 1 or 100 atm O_2 (for 24 h with rapid cooling to room temperature).

tion of the $YBaCo_4O_{7+\delta}$ phase. Note that this is not straightforwardly expected from the fact that the phase was successfully obtained in pure form through synthesis at 1200 °C in air. Apparently, in the Y−Ba−Co−O system, the $YBaCo_4O_{7+\delta}$ phase is thermodynamically stable only at relatively high temperatures (>900 °C in air); at low temperatures, it is then kinetically stabilized (as a metastable phase) provided that the cooling rate over the temperature range of 600∼900 °C is fast enough to prevent its decomposition into $BaCoO_{3-\delta}$ (plus *debris*). At 500 °C, the decomposition is already hindered by the kinetics: all the samples obtained through annealing the as-synthesized material in O_2 at 500 °C for periods of 1−24 h were of single-phase $YBaCo_4O_{7+\delta}$ with the lattice parameters essentially identical to those of the as-synthesized sample. Also, the oxygen contents of these samples were confirmed to equal that of the as-synthesized sample within experimental error limits.

The origin of the first (lower-temperature) weight gain-and-loss hump at about 200∼400 °C (Figure 2) was found to reflect a unique ability of the $YBaCo_4O_{7+\delta}$ phase to reversibly absorb and release oxygen in the said temperature range. The XRD patterns collected for samples after O_2 or air annealing at temperatures below 500 °C showed no indication of any decomposition of the $YBaCo_4O_{7+\delta}$ phase. During the TG runs carried out at a heating rate of 1 °C/min, the maximum oxygen content reached in air was $7 + \delta \approx 8.0$, as seen from Figure 2. In O_2, a slightly higher value of $7 + \delta \approx 8.2$ was achieved. The real equilibrium oxygen-content values were revealed from the longer (24-hour) postannealing treatments performed for the as-synthesized $YBaCo_4O_{7.01}$ powder at various temperatures in flowing O_2 gas (with a rapid cooling back to room temperature). Additionally, we performed oxygenation annealings in 100 atm O_2 in the temperature range of 240∼390 °C. All the postannealed samples were confirmed to remain nondecomposed by XRD. Their oxygen contents were analyzed by iodometric titration, the results being summarized in Figure 3. These data show that the maximum oxygen content reached for samples annealed in 1 atm O_2 is $7 + \delta \approx 8.3$, whereas it slightly exceeds 8.5 for those annealed in 100 atm O_2. Accordingly, the Co valence $V(Co)_{av}$ increases up to ∼3. The oxygen-content variation range in $YBaCo_4O_{7+\delta}$ is unusually wide. That is, an amount of oxygen that corresponds to ∼20% of the total oxygen content is readily loaded or removed, being triggered by just a tiny change in temperature or atmosphere. To our knowledge, no other oxide shows comparable characteristics.

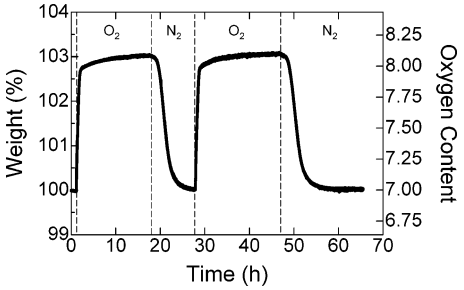

Figure 4. Isothermal TG curve recorded for $YBaCo_4O_{7+\delta}$ at 350 °C upon switching the gas flow from N_2 to O_2 and vice versa.

In both atmospheres, air and O_2, a weak trend of decreasing equilibrium oxygen-content value with increasing temperature is discerned from Figure 3. This is along the characteristics common to all metal oxides: the lower the temperature, the higher the equilibrium oxygen content under a fixed oxygen partial pressure.[6] (In other words, the Gibbs energy of formation becomes less negative as temperature increases.[27]) On the other hand, from Figure 2, the major oxygen loss from $YBaCo_4O_{7+\delta}$ upon heating in O_2 occurs in a single, very sharp step at about 400 °C. We also investigated the oxygen-depletion process in N_2 (thermogram not shown): in this inert atmosphere, the excess oxygen is lost in an even sharper process at a somewhat lower temperature, ∼360 °C. Attempts to obtain samples with $0.0 < \delta < 1.2$ by means of longer-period annealing in N_2 at temperatures between 280 and 360 °C all ended up with a depletion of oxygen down to the $\delta \approx 0$ level. This is in contrast to the oxygen-depletion behavior seen for many other oxygen-nonstoichiometric transition-metal oxides, such as $RBa_2Cu_3O_{6+\delta}$ (R = rare earth element; triple perovskite; $0 < \delta < 1$), $RBaCo_2O_{5+\delta}$ (double perovskite; $0 < \delta < 0.7$), and $LaCuO_{3-\delta}$ (perovskite; $0 < \delta < 0.5$), from which the excess-oxygen release in N_2 occurs gradually in the temperature range of approximately 300∼800 °C.[6,23,26]

Keeping an eye on possible applications of $YBaCo_4O_{7+\delta}$ that make use of its unusual low-temperature oxygen absorption/desorption capability, we first confirmed the reversibility of the phenomenon. Figure 4 shows isothermal TG data for $YBaCo_4O_{7+\delta}$ at 350 °C upon switching the gas flow from N_2 to O_2 and vice versa. It is seen that the resultant oxygen incorporation and depletion processes occur in a highly reversible manner. The seemingly slower response of the O_2-to-N_2 shift in comparison to the stimulus of the opposite shift is well-explained by the fact that the time scale for oxygen removal from the sample chamber is significant when the atmosphere is changed from O_2 to N_2. We, moreover, investigated the dependence of the speed of oxygen incorporation (after switching the gas flow from N_2 to O_2) on the annealing temperature (in the range from 270 to 350 °C). The resultant TG curves are displayed in Figure

(27) Richardson, F. D.; Jeffes, J. H. E. *J. Iron Steel Inst., London* **1948**, *160*, 261.

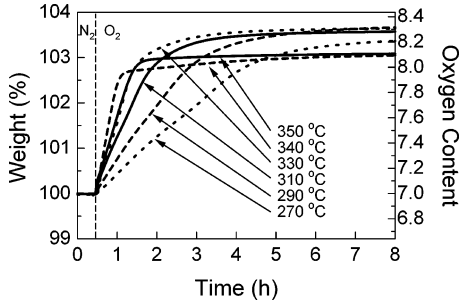

Figure 5. Isothermal TG curves recorded at different temperatures for oxygen-depleted $YBaCo_4O_{7+\delta}$ after switching the gas flow from N_2 to O_2.

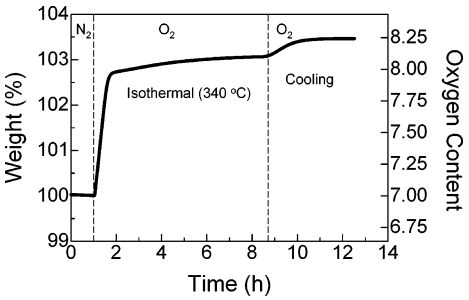

Figure 6. TG curve recorded for oxygen-depleted $YBaCo_4O_{7+\delta}$ upon isothermal oxygen loading in O_2 at 350 °C and subsequent slow cooling (cooling rate 1 °C/min) in O_2.

5. As expected, the incorporation rate increases with increasing temperature, though most profoundly only up to 330 °C. Then, above 330 °C, the maximum amount of oxygen taken by the $YBaCo_4O_{7+\delta}$ lattice starts to decrease. This observation is consistent with our earlier discussion on the basis of the equilibrium oxygen content values given in Figure 3. Even more clearly, the same conclusion is revealed from the TG curve shown in Figure 6 for a process in which $YBaCo_4O_{7+\delta}$ is first oxygenated during isothermal O_2 annealing at 340 °C and then slowly cooled to room temperature in an O_2 flow: the value achieved for the oxygen content at 340 °C yet increases markedly during the slow cooling process.

From the XRD patterns given in Figure 7 for two representative $YBaCo_4O_{7+\delta}$ samples with $\delta = 0.01$ and 1.25, it seems that the oxygen incorporation process is topotactic; that is, the crystal structure remains essentially the same. There are no clearly distinguishable peaks for the $\delta = 1.25$ sample that would not fit a similar hexagonal cell as for the $\delta = 0.01$ sample. One may thus envisage that the heavy cations are not significantly displaced from their (ortho)-hexagonal sites. However, some of the diffraction peaks for the $\delta = 1.25$ sample show additional broadening/splitting, indicating a possible change in symmetry. The possible change in space group could, however, not be determined on the basis of the present XRD data only. Moreover, the data are not sufficiently sensitive for extracting data for the location of the incorporated oxygen atoms in the structure. Therefore, we have initiated a detailed neutron diffraction and high-resolution electron microscopy and diffraction study to clarify the fine-structure of the oxygenated form of $YBaCo_4O_{7+\delta}$. Here, we tentatively derived the lattice parameters for the $\delta = 1.25$ sample from the present XRD data using space group $P6_3mc$ such that $a = 6.311(1)$ Å and

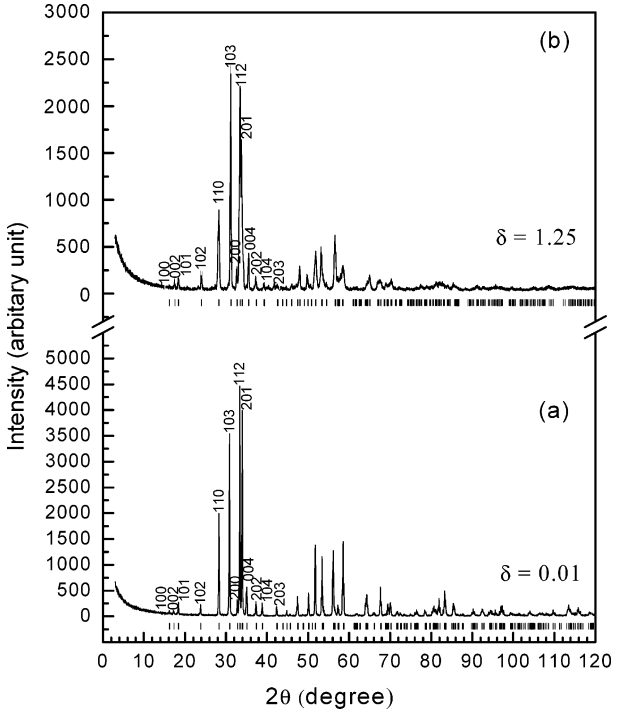

Figure 7. X-ray diffraction patterns together with allowed Bragg reflection positions in space group $P6_3mc$ (vertical bars) for two $YBaCo_4O_{7+\delta}$ samples with $\delta =$ (a) 0.01 and (b) 1.25. In addition, Miller indices for the first 13 reflections are given.

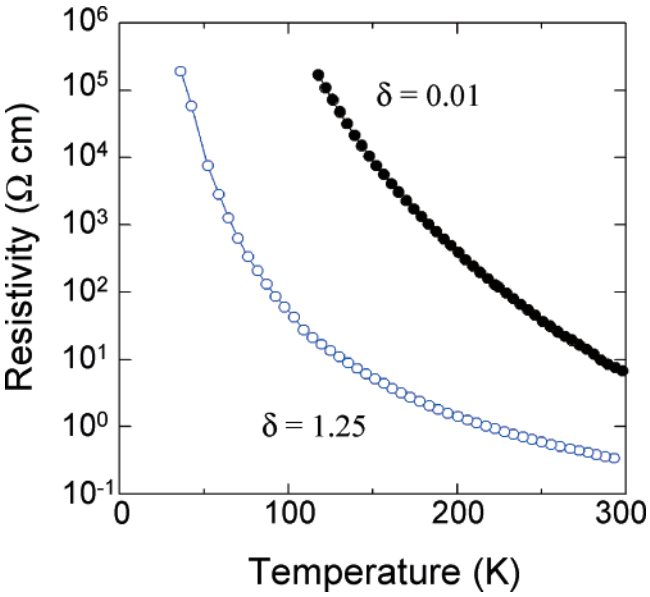

Figure 8. Temperature dependence of resistivity for two $YBaCo_4O_{7+\delta}$ samples with $\delta = 0.01$ and 1.25.

$c = 10.106(1)$ Å. A comparison of the lattice parameters to those of the $\delta \approx 0$ form [$a = 6.300(1)$ Å and $c = 10.237(1)$ Å] reveals that, upon oxygen incorporation, the c parameter shrinks whereas the a parameter slightly elongates. Using the lattice parameters and the tabulated Shannon ionic radii,[28] we furthermore estimated the volume fraction filled with the constituent atoms/ions (assuming that they are nonpenetrating and incompressible spheres) as follows: 59% for $\delta = 0.01$ and 68% for $\delta = 1.25$. (Just for a rough comparison, using the published crystal structure data,[29] the corresponding

(28) Shannon, R. S. *Acta Crystallogr.* **1976**, *A32*, 751.

values for another transition-metal oxide, $YBa_2Cu_3O_{6+\delta}$, with a relatively wide-range oxygen-content tunability become 64% for $\delta \approx 0$ and 68% for $\delta \approx 1$.) Thus, we conclude that the rather open $YBaCo_4O_7$ structure possesses space wide enough to allow extra-oxygen incorporation.

Finally, Figure 8 presents resistivity versus temperature curves for $YBaCo_4O_{7+\delta}$ with oxygen contents, $\delta = 0.01$ and 1.25, both exhibiting a semiconductor-like $\rho(T)$ dependence. Oxygen loading decreases the absolute resistivity values markedly, suggesting that $YBaCo_4O_{7+\delta}$ is a hole-doped system. This is consistent with the fact that the Seebeck coefficient was found to be positive for both the compositions. The room-temperature S values were ~190 and ~150 μV/K for the $\delta = 0.01$ and 1.25 samples, respectively, the lower value for the latter sample being in accordance with the higher hole-doping level. From the ρ versus T data, the activation energy was found to decrease from 0.28 eV for $\delta = 0.01$ to 0.10 eV for $\delta = 1.25$. We also note that the fully oxygenated $YBaCo_4O_{8.5}$ composition with Co in an average valence state of 3 is anticipated to be interesting from the magnetic point of view. This will be addressed in our near-future works.

(29) Jorgensen, J. D.; Veal, B. W.; Paulikas, A. P.; Nowicki, L. J.; Crabtree, G. W.; Claus, H.; Kwok, W. K. *Phys. Rev. B* **1990**, *41*, 1863. Cava, R. J.; Hewat, A. W.; Hewat, E. A.; Batlogg, B.; Marezio, M.; Rabe, K. M.; Krajewski, J. J.; Peck, W. F., Jr.; Rupp, L. W., Jr. *Physica C* **1990**, *165*, 419.

Conclusion

We have presented a new cation-stoichiometric oxide framework, that is, the $YBaCo_4O_{7+\delta}$ system, which allows reversible oxygen loading and subsequent low-temperature discharging. The swinging between the oxygen-depleted and the oxygen-loaded situation is controlled by modest changes in temperature or oxygen partial pressure. The system absorbs oxygen up to $\delta \approx 1.5$ upon low-temperature (270~350 °C) heating in an O_2-containing atmosphere and sharply releases the oxygen, even in an O_2 atmosphere, when the temperature exceeds ~400 °C. (Needless to say, the very exact temperature naturally depends on the partial pressure of oxygen.) These unique characteristics are clearly beyond those of known nonstoichiometric oxides in terms of both the magnitude and the sharpness of the absorption/desorption process, thus making the $YBaCo_4O_{7+\delta}$ system a highly potential material candidate for various applications based on reversible oxygen storage. It is even possible that utilization of the unique oxygen absorption/desorption ability of $YBaCo_4O_{7+\delta}$ might open totally new applications.

Acknowledgment. This work was supported by Grants-in-Aid for Scientific Research (Nos. 15206002 and 15206071) from the Japan Society for the Promotion of Science and by the Research Council of Norway, Grant No.158518/431 (NANOMAT).

CM0523081